Accurate estimation of the near-Sun magnetic field of Coronal Mass Ejections
with the use of magnetic helicity

K. Moraitis[1], E. Pariat[1], A. Savcheva[2]
[1] LESIA, Observatoire de Paris, [2] Harvard-Smithsonian Center for Astrophysics
kostas.moraitis@obspm.fr

l'Observatoire de Paris — LESIA
Laboratoire d'Études Spatiales et d'Instrumentation en Astrophysique

Harvard-Smithsonian Center for Astrophysics

Introduction

Interplanetary Coronal Mass Ejections (CMEs) and their subset of Magnetic Clouds (MCs) are of great importance to Space Weather since they can produce geomagnetic storms. One of the parameters determining the strength of the storm is the value of the MC's magnetic field close to the Sun [1], a few solar radii from its surface (Fig. 1).

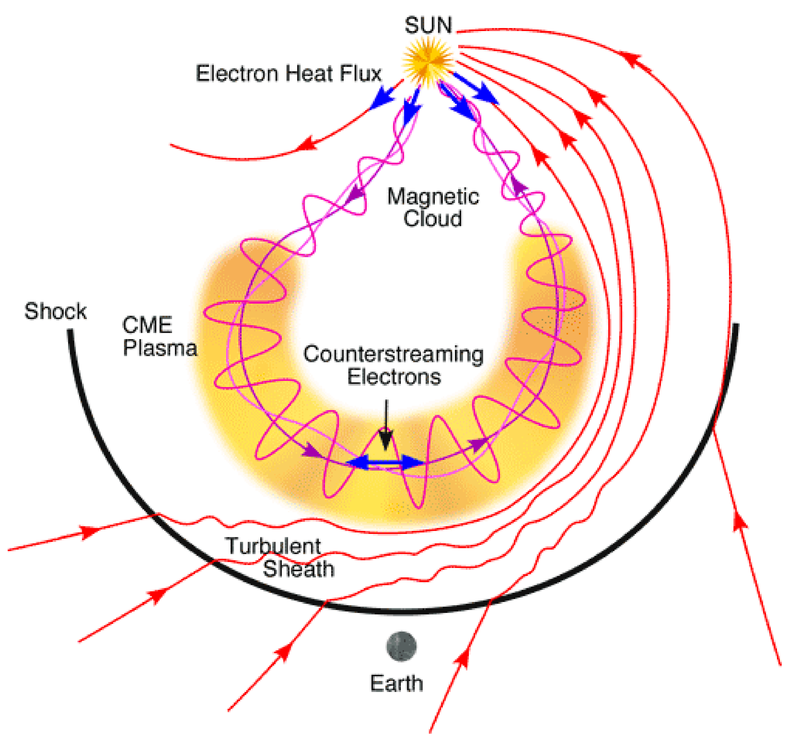

Figure 1: Schematic of a Magnetic Cloud and its components (from NASA's cosmos).

The simplest model for the magnetic field of a MC is the axially symmetric, linear force-free Lundquist configuration [2], given by

$$B(r,\varphi,z) = B_0\left(J_1\left(2.405\frac{r}{R}\right)\hat{\varphi} + J_0\left(2.405\frac{r}{R}\right)\hat{z}\right) \quad (1)$$

z : axis of MC; r, φ, z: cylindrical coordinates
R : radius of MC; J_0, J_1: Bessel functions
B_0: magnetic field strength at the MC axis

The relative magnetic helicity, H, for this magnetic field, if we consider a part of the MC with length L along its axis, is [3]

$$H = 0.7 B_0^2 R^3 L \quad (2)$$

Solving for the magnetic field (MF) strength we get

$$B_0 = \left(\frac{H}{0.7R^3L}\right)^{1/2} \quad (3)$$

The magnetic field strength B_0 thus depends on the parameters H, R, and L. The latter two are geometrical relating to the shape of the MC. For the geometrical description of a CME – MC we follow the Graduated Cylindrical Shell (GCS) model [4], shown in Fig. 2.

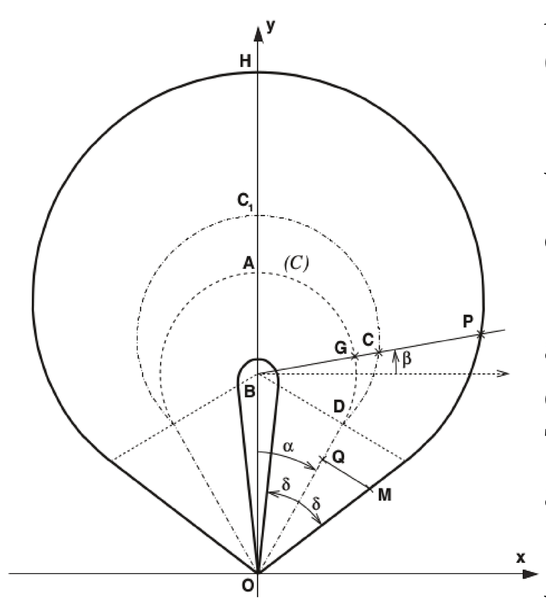

Figure 2: Basic geometrical parameters of the Graduated Cylindrical Shell model (from [3]).

According to this, the MC radius (HC_1 in Fig. 2) is given by

$$R = \kappa \cdot r_{ax} \quad (4)$$

where r_{ax} is the heliocentric distance of the MC's axis (OC_1), and

$$\kappa = \sin\delta$$

a parameter relating to the angular extent of the legs of the CME.
The length of the MC along its axis is

$$L = 2\alpha \cdot r_{ax} \quad (5)$$

where 2α is the CME angular extent.
Replacing Eq. (5) in Eq. (3) we get:

$$B_0 = 0.24\ \mathrm{G}\left(\frac{H}{10^{42}\ \mathrm{Mx}^2}\right)^{1/2}\left(\frac{R}{R_\odot}\right)^{-3/2}\left(\frac{\alpha}{30^\circ}\right)^{-1/2}\left(\frac{r_{ax}}{R_\odot}\right)^{-1/2} \quad (6)$$

a relation consistent with the results of [5]. The relative magnetic helicity of the MC however cannot be inferred directly. For this we assume that the MC helicity is that of the active region (AR) where the CME originated, since helicity is a conserved quantity [6, 7], and treat this as an upper limit.

Helicity calculation method

Relative magnetic helicity of a magnetic field, B, is defined by [8]

$$H = \int_V (A + A_p)\cdot(B - B_p)\,dV \quad (7)$$

B_p: potential (current-free) magnetic field
A, A_p: vector potential of B, B_p

Relative magnetic helicity is independent of the gauges chosen for the vector potentials (aka physically meaningful), as long as

$$\hat{n}\cdot B\big|_{\partial V} = \hat{n}\cdot B_p\big|_{\partial V} \quad (8)$$

Helicity is calculated from Eq. (7) by extending a previously developed method in Cartesian coordinates [9, 10], into the spherical geometry. The method works in two steps:

Step 1: Potential magnetic field calculation

The potential magnetic field $\mathbf{B}_\mathrm{p} = \nabla\Phi$ is obtained from a scalar potential that satisfies Laplace's equation $\nabla^2\Phi = 0$
We consider wedge-shaped volumes (as in Fig. 3) of the form

$$V = \{(r,\theta,\varphi): r\in[r_{min}, r_{max}], \theta\in[\theta_{min},\theta_{max}], \varphi\in[\varphi_{min},\varphi_{max}]\}$$

After taking into account the condition of Eq. (8), the Boundary Value Problem we have to solve is

$$\frac{1}{r^2}\frac{\partial}{\partial r}\left(r^2\frac{\partial\Phi}{\partial r}\right) + \frac{1}{r^2\sin\theta}\frac{\partial}{\partial\theta}\left(\sin\theta\frac{\partial\Phi}{\partial\theta}\right) + \frac{1}{r^2\sin\theta^2}\frac{\partial^2\Phi}{\partial\phi^2} = 0$$

$$\frac{\partial\Phi}{\partial\hat{n}}\bigg|_{\partial V} = \hat{n}\cdot\mathbf{B}|_{\partial V} \quad (9)$$

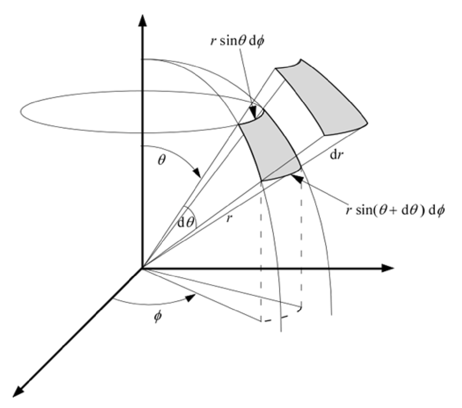

Figure 3: Example of an elementary volume in spherical coordinates.

We use the MUDPACK library for the solution of Laplace's equation that employs a multigrid technique which is computationally fast and robust.

Step 2: Vector potentials calculation

Given B (B_p) the respective vector potential is obtained by the solution of $\mathbf{B} = \nabla\times\mathbf{A}$ for A (A_p).
Using the DeVore gauge, $\boldsymbol{A_r=0}$, we have

$$\mathbf{A}(r,\theta,\phi) = \frac{1}{r}\left(r_0\boldsymbol{\alpha}(\theta,\phi) + \hat{\mathbf{r}}\times\int_{r_0}^{r}\mathrm{d}r'\,r'\mathbf{B}(r',\theta,\phi)\right)$$

$$\nabla_\perp\times\boldsymbol{\alpha} = \frac{1}{r_0\sin\theta}\left(\frac{\partial}{\partial\theta}(\sin\theta\alpha_\phi) - \frac{\partial\alpha_\theta}{\partial\phi}\right) = B_r(r_0,\theta,\phi) \quad (10)$$

- The reference plane r_0 can be chosen as the top or the bottom one
- Additionally, the vector potential on this plane, $\boldsymbol{\alpha}$, can be in the following gauges

DeVore Simple Gauge

$$\alpha_\phi(\theta,\phi) = \frac{cr_0}{\sin\theta}\int_{\theta_0}^{\theta}\mathrm{d}\theta'\,\sin\theta' B_r(r_0,\theta',\phi)$$

$$\alpha_\theta(\theta,\phi) = -(1-c)r_0\sin\theta\int_{\phi_0}^{\phi}\mathrm{d}\phi'\,B_r(r_0,\theta,\phi') \quad (11)$$

DeVore Coulomb Gauge

$$\boldsymbol{\alpha} = \hat{\mathbf{r}}\times\nabla_\perp u = \frac{1}{r_0}\left(-\frac{1}{\sin\theta}\frac{\partial u}{\partial\phi}, \frac{\partial u}{\partial\theta}\right)$$

$$\nabla_\perp\boldsymbol{\alpha} = 0 \quad (12)$$

$$\nabla_\perp^2 u = B_r(r_0,\theta,\phi)$$

The vector potentials are thus obtained by simple integrations, and optionally, by the solution of a 2D Poisson problem.

Helicity computation: Method validation

Our method is tested with the semi-analytic, force-free magnetic field solutions of [11]. We use the n=m=1 case of LL with the source placed 30 Mm below the photosphere and rotated by π/4 with respect to the radial direction. The LL field extents 20ºx20º in the θ-φ plane, and 200 Mm in height (Fig. 4).

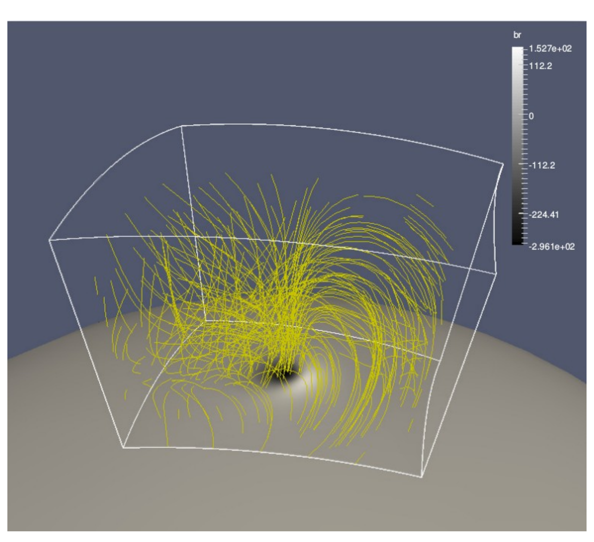

Figure 4: Morphology of the magnetic field used in testing the helicity calculation method.

field	grid	$\langle\lvert f_i\rvert\rangle$	ϵ_{flux}	ξ
$\mathbf{B}$	129	$2.21\,10^{-4}$	$1.70\,10^{-3}$	$1.99\,10^{-2}$
$\mathbf{B_p}$		$1.15\,10^{-4}$	$1.83\,10^{-3}$	$1.81\,10^{-4}$
$\mathbf{B}$	257	$2.16\,10^{-4}$	$2.15\,10^{-3}$	$3.67\,10^{-2}$
$\mathbf{B_p}$		$2.14\,10^{-4}$	$2.23\,10^{-3}$	$3.59\,10^{-4}$

Table 1: Solenoidality ($\lvert f_i\rvert$, ε_{flux}), and force-freeness (ξ) metrics for the original and the respective potential fields in two different resolutions.

- The produced potential field is solenoidal and force-free to a large degree (Table 1), and satisfies condition of Eq. (8) well (Fig. 5).
- The vector potentials reproduce the respective magnetic fields equally well in DVS and DVC gauges, and better when the top boundary is taken as reference plane than the bottom (Table 2).

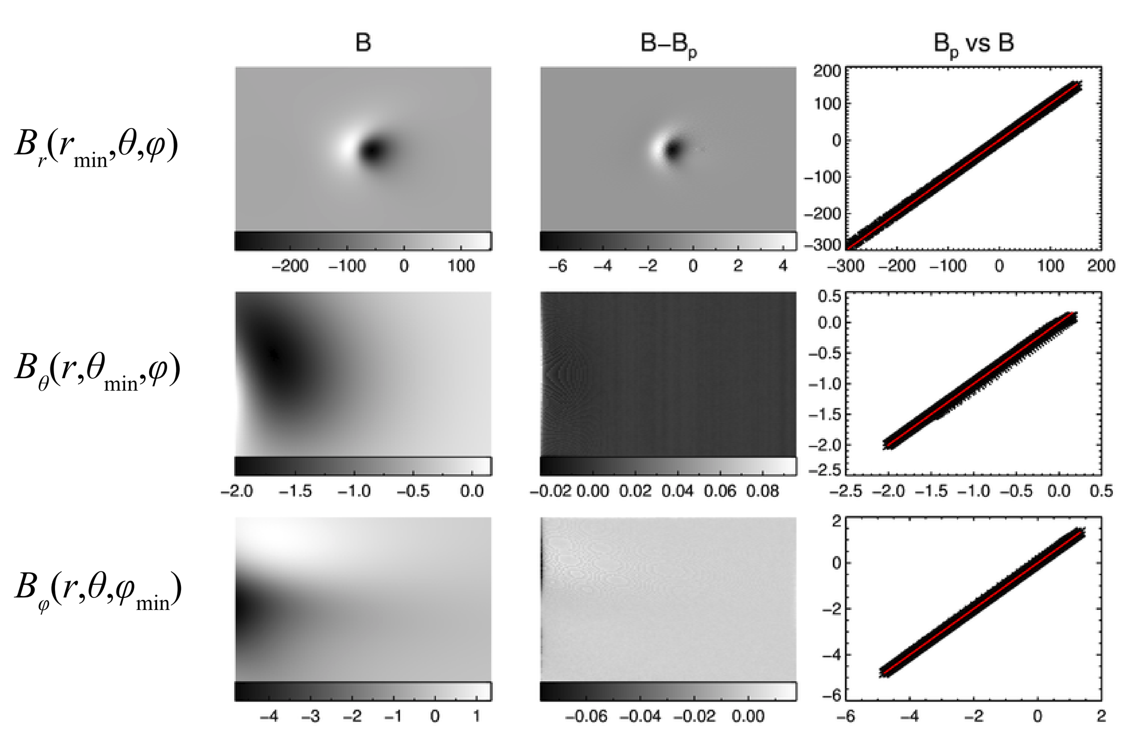

Figure 5: Comparison of original and respective potential fields in three out of the six boundaries of the considered volume.

Table 2: Reconstruction metrics for the original and the potential magnetic field computed in various gauges and different resolutions.

field	gauge	grid	correlation coefficients of $\mathbf{B}$ vs $\nabla\times\mathbf{A}$: B_r	B_θ	B_ϕ	Schrijver metrics: C_{vec}	C_{CS}	E'_{n}	E'_{m}	ϵ
$\mathbf{B}$	DVSt	129	0.9999	1.0000	1.0000	0.9999	1.0000	0.9948	0.9959	0.9980
	DVSt	257	0.9999	1.0000	1.0000	0.9999	1.0000	0.9942	0.9949	0.9986
	DVSb	129	0.9990	1.0000	1.0000	0.9995	0.9986	0.9814	0.9613	1.0025
	DVCt	129	0.9999	1.0000	1.0000	0.9999	0.9999	0.9947	0.9953	0.9980
$\mathbf{B_p}$	DVSt	129	1.0000	1.0000	1.0000	1.0000	0.9997	0.9884	0.9816	0.9998
	DVSt	257	0.9995	1.0000	1.0000	0.9997	0.9962	0.9568	0.9283	0.9993
	DVSb	129	0.9990	1.0000	1.0000	0.9995	0.9920	0.9727	0.9441	0.9901
	DVCt	129	1.0000	1.0000	1.0000	1.0000	0.9997	0.9883	0.9814	0.9998

Application to a synthetic eruption

We use the data-driven nonlinear force-free reconstruction of the magnetic field of NOAA AR 11060 by [12]. This uses the flux-rope (FR) insertion method to model the AR. The inserted flux rope is relaxed towards force-free state with a magnetofrictional method. From the evolution shown in Fig. 6, we see that the flux rope moves upwards and finally erupts during the relaxation.

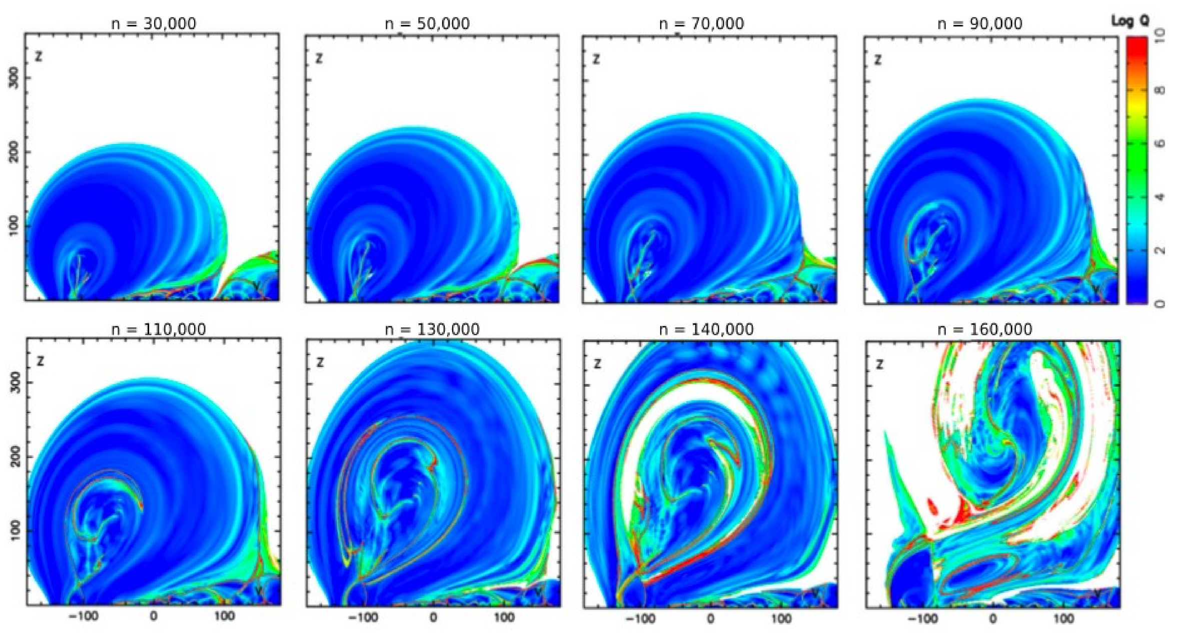

Figure 6: Selected snapshots of a cross section of the Quasi Separatrix Layer map during the MF relaxation of NOAA AR 11060 [12], as quantified by the squashing factor Q. The flux rope moves upwards and finally crosses the upper plane in an eruptive-like manner. Axes units are Mm.

For the snapshot at 130000 iterations we see in Fig. 6 that the flux-rope radius is R=100 Mm, while its axis is at the height h=150 Mm above the solar surface. Using the helicity calculation method described before, we compute the instantaneous value of helicity for each snapshot during the relaxation of the magnetic field.

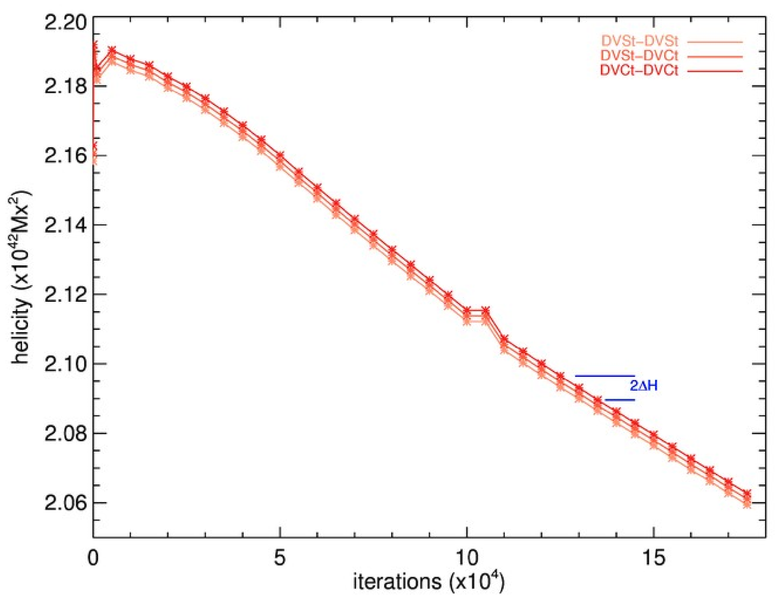

Figure 7: Evolution of the relative magnetic helicity during the relaxation of the magnetic field, computed with three different gauge combinations for the vector potentials A and A_p. The very good agreement between the three curves indicates that the developed helicity calculation method is quite accurate. Also shown is the helicity change at the time of 130000 iterations.

- From the evolution of the AR's helicity in Fig. 7 we get the upper limit ΔH=3.4·10^{39} Mx^2 for the helicity change at the specific time. Inserting this helicity value in Eq. (6) for the CME MF, the flux-rope radius R, the heliocentric distance of the FR axis, $r_{ax}=R_\odot+h$, and assuming α=30º, we estimate

  B_0 = 0.24 G

- On the other hand, the average horizontal MF strength at the height of the flux rope h at 130000 iterations is

  B_0 = 1.01 G

  and ranges in [0.3 G, 2 G]. Alternatively, the inserted flux rope has an axial flux of Φ_{axi}=6·10^{20} Mx [12], which for the given radius R, translates to the MF strength

  B_0 = 0.48 G

  The agreement is thus reasonable given all the uncertainties.

Conclusions

- Magnetic helicity can be used to estimate the CME magnetic field strength, a quantity important for Space Weather
- The accurate estimation of helicity is essential in this goal
- We developed a method to properly compute (relative magnetic) helicity in spherical coordinates
- Application of the method to a synthetic eruption determines the CME MF reasonably well

References

1. Wu & Lepping 2005, J. Atmos. & Sol. Ter. Phys., 67, 28
2. Lundquist 1950, Ark. Fys., 2, 361
3. Dasso et al. 2006, A&A, 455, 349
4. Thernisien, Howard & Vourlidas 2006, ApJ, 652, 763
5. Patsourakos & Georgoulis 2016, A&A, 595, A121
6. Woltjer 1958, Proc. Nat. Acad. Sciences, 44, 489
7. Taylor 1974, PRL, 33, 1139
8. Finn & Antonsen 1985, Comm. Plasma Phys. & Contr. Fusion, 9, 111
9. Valori, Démoulin & Pariat 2012, Sol. Phys., 278, 347
10. Moraitis et al. 2014, Sol. Phys., 289, 4453
11. Low & Lou 1990, ApJ, 352, 343
12. Savcheva et al. 2016, ApJ, 817, 43

PROJET FINANCÉ PAR L'ANR – PROJECT FUNDED BY THE ANR
HELISOL